[Frontiers in Bioscience S2, 454-467, January 1, 2010]

Characterization of a three-drug nonlinear mixture response model

Yseult Françoise Brun[1,2] , William R. Greco[1,2]

[1]Division of Cancer Prevention and Population Sciences, Roswell Park Cancer Institute, Buffalo, NY 14263; [2]School of Pharmacy and Pharmaceutical Sciences, University at Buffalo, SUNY, Buffalo, NY 14260

TABLE OF CONTENTS

1. ABSTRACT

Our group recently developed a response-surface modeling paradigm (White *et al*: Curr Drug Metab 2, 399-409, 2003) and tested its application to both mixtures of anticancer agents and antifungals. This new model is a Hill-type equation, with the slope and potency parameters being functions of the normalized drug ratios, using polynomial expressions. Response surface methods allow one to model and interpret all of the information present in the full concentration-effect data set, to visualize local regions of synergy, additivity and antagonism, and even to quantify the degree of synergy or antagonism, both globally, and across local regions of the response surface. In the present article, we study the effect of changes in the different parameters of the polynomial expressions for two-drug and three-drug mixtures, on the geometrical shapes of several 2-dimensional representations of the 3-dimensional concentration-effect surface. A secondary goal of this report is to compare the mathematical characteristics of the rival White and (Minto *et al*: Anesthesiol 92, 1603-1616, 2000) modeling paradigms.

2. INTRODUCTION

In the past, many varied approaches to the assessment of synergy, additivity and antagonism have been developed and applied to real data (1). They include older numerical (e.g., 2) and graphical (e.g., 3) methods and older statistical response surface methods (e.g., 4). The older response surface methods are mostly limited to two-agent interactions (e.g., 4) or have other limitations, but some newer response surface methods can be used for three-agent and higher order combinations (e.g., 5-8).

Response surface methods allow one to model and interpret all of the information present in the full concentration-effect data set, to visualize local regions of synergy, additivity and antagonism, and even to quantify the degree of synergy or antagonism, both globally, and across local regions of the response surface.

Such information from in-vitro studies can be useful to pinpoint which drug combinations may be good candidates for further in-vivo studies, and subsequent

clinical studies. In addition, this information may also help to suggest optimal proportions of the agents.

In this article we use Loewe additivity [defined in (1)] as the standard for defining "no interaction" among several drugs. The response surface model studied here reduces to Loewe additivity in the complete absence of synergy or antagonism. The model has already been presented in the literature for use with both combinations of anticancer drugs (5-6) and antifungals (7). This new model is a Hill-type equation, with the steepness and potency parameters being functions of the normalized drug ratios, using polynomial expressions. For examples of how our main model (equation 1 described in Section 3) has been fit to real laboratory data, and how we have dealt with the statistical complexities of experimental design, curve fitting, model building, and results interpretation, the reader is encouraged to peruse our three published applications (5-7). The current article showcases the mathematical characteristics of the model, in order to provide the potential user with a good geometrical understanding of the model structure and parameters. This type of geometrical understanding is critical for a deep biological understanding of results from fitting real data with the model.

Minto *et al.* (8) published an interaction model three years before we independently, without knowledge of the former work, published the White model (5). The two models have many similarities; we will compare and contrast the Minto and White models.

Both the Minto (8) and White (5) drug combination models have advantages over older drug combination response surface models (e.g., 1, 4). Both of these newer modeling paradigms allow: (a) local regions of synergism and antagonism throughout the multidimensional surface; (b) extreme antagonism; (c) more than 2 drugs to be modeled simultaneously; (d) complex patterns of other concentration-effect parameters (Econ, B%, m; explained below in equation 1). The disadvantages of the two newer models is that their increased complexities require larger experiments, more complex model-building routines, and more complex explanations of the results.

A secondary goal of this report is to compare the mathematical characteristics of the rival Minto (8) and White (5) modeling paradigms.

3. MAIN MATHEMATICAL MODEL

The overall response surface model that we will study is essentially a 4-parameter Hill model with polynomial expressions replacing the steepness m and potency CI_{50} parameters:

(equation 1)

$$E(\mathbf{X},T,\boldsymbol{\theta}) = \frac{\left[Econ - \frac{B\%\,Econ}{100}\right]\left(\frac{T}{CI_{50}(\mathbf{X},\boldsymbol{\theta})}\right)^{m(\mathbf{X},\boldsymbol{\theta})}}{1+\left(\frac{T}{CI_{50}(\mathbf{X},\boldsymbol{\theta})}\right)^{m(\mathbf{X},\boldsymbol{\theta})}} + \frac{B\%\,Econ}{100}$$

With

E: the measured endpoint (or effect or response or output or dependent variable).
Econ: the measured endpoint at zero drug concentration (control).
B%: the measured endpoint at infinite concentration(s) (the background endpoint, expressed as a percentage of Econ).
m: the steepness function (expression).
CI_{50}: combination index expression (normalized potency expression) at the 50% level.
X represents the vector of normalized fractions of each drug. For example, for drug A

$$X_A = \frac{C_A / IC_{50,A}}{T} \qquad \text{(equation 2)}$$

in which $IC_{50,A}$ represents the median effective dose (or concentration) of drug A,

and T represents the total normalized amount of drug in the mixture

(equation 3)

$$T = C_A / IC_{50,A} + C_B / IC_{50,B} + C_C / IC_{50,C}$$

(as an example for a three drug mixture).

The ms and CI_{50}s are modeled as functions of drug fractions, using the following constrained polynomials. When dealing with two-drug mixtures:

For m (equation 4)

$$m(\mathbf{X},\boldsymbol{\theta}) = (\alpha_{m1} * X_A) + (\alpha_{m2} * X_B) + (\beta_{m12} * X_A * X_B) + (\gamma_{m12} * X_A * X_B * (X_A - X_B))$$

For CI_{50}: (equation 5)

$$CI_{50}(\mathbf{X},\boldsymbol{\theta}) = 10\text{^}\{(1-X_A)*(1-X_B)* [(\alpha_{D1} * X_A) + (\alpha_{D2} * X_B) + (\beta_{D12} * X_A * X_B) + (\gamma_{D12} * X_A * X_B * (X_A - X_B))]\}$$

When dealing with three-drug mixtures:
For m (equation 6)

$$m(\mathbf{X},\boldsymbol{\theta}) = (\alpha_{m1} * X_A) + (\alpha_{m2} * X_B) + (\alpha_{m3} * X_C) + (\beta_{m12} * X_A * X_B) + (\beta_{m13} * X_A * X_C) + (\beta_{m23} * X_B * X_C) + (\gamma_{m12} * X_A * X_B * (X_A - X_B)) + (\gamma_{m13} * X_A * X_C * (X_A - X_C)) + (\gamma_{m23} * X_B * X_C * (X_B - X_C)) + (\delta_{m123} * X_A * X_B * X_C)$$

Table 1. Polynomial coefficients for complex CI_{50} patterns with two drugs

	Curve Label							
Parameter	A1	A2	A3	A4	A5	A6		
α_{D1}	-10	-3	-3	-10	-40	-40		
α_{D2}	-3	-10	-10	-3	-40	-40		
β_{D12}	0	0	0	0	150	150		
γ_{D12}	50	-50	-80	80	80	-80		
	B1	B2	B3	B4	B5	B6		
α_{D1}	10	3	3	10	40	40		
α_{D2}	3	10	10	3	40	40		
β_{D12}	0	0	0	0	-150	-150		
γ_{D12}	-50	50	80	-80	-80	80		
	C1	C2	C3	C4	D1	D2	D3	D4
α_{D1}	-30	7	30	-7	40	-40	-20	20
α_{D2}	7	-30	-7	30	20	-20	-40	40
β_{D12}	40	40	-40	-40	-150	150	150	-150
γ_{D12}	30	-30	-30	30	-60	60	-60	60
	E1	E2						
α_{D1}	40	-40						
α_{D2}	40	-40						
β_{D12}	-195	195						
γ_{D12}	0	0						

The table lists the polynomial coefficients used for simulating the CI_{50}s in Figure 13 through Figure 22 with equation 5. Labels A1 to E2 are for the different curves in the figures.

Table 2. Polynomial coefficients for complex m patterns with two drugs

	Curve Label							
Parameter	A1	A2	A3	A4	B1	B2	B3	B4
α_{m1}	-2	-2	-0.5	-0.5	-2	-2	-0.5	-0.5
α_{m2}	-0.5	-0.5	-2	-2	-0.5	-0.5	-2	-2
β_{m12}	-9	3.5	-9	4.5	2.5	-2.5	2.5	-2.5
γ_{m12}	6	-2	6	-2	2	2	-2	-2

The table lists the polynomial coefficients used for simulating the ms in Figure 25 (curves A1 to A4) and Figure 26 (B1 to B4) with equation 4. Labels A1 to B4 are for the different curves in the figures.

For CI_{50}:

(equation 7)

$$CI_{50}(\mathbf{X},\boldsymbol{\theta}) = 10\text{^}\{(1-X_A)*(1-X_B)*(1-X_C)*[(\alpha_{D1}*X_A)+(\alpha_{D2}*X_B)+(\alpha_{D3}*X_C)+(\beta_{D12}*X_A*X_B)+(\beta_{D13}*X_A*X_C)+(\beta_{D23}*X_B*X_C)+(\gamma_{D12}*X_A*X_B*(X_A-X_B))+(\gamma_{D13}*X_A*X_C*(X_A-X_C))+(\gamma_{D23}*X_B*X_C*(X_B-X_C))+(\delta_{D123}*X_A*X_B*X_C)]\}$$

All of the α, β, γ and δ terms are polynomial coefficients (estimatible parameters).

We will particularly focus on the patterns that m and CI_{50} functions can take depending on the values of the polynomial coefficients α, β, γ and δ. For each specific group of drugs, α, β, γ and δ form the vector **θ** referenced in equation 1.

4. RESULTS AND DISCUSSION

In this section, we will discuss patterns obtained by changing the various polynomial coefficients α, β, γ and δ, first by varying each single polynomial coefficient by a systematic increment, while fixing the other coefficients at zero; and second by varying two or more coefficients simultaneously.

For two-drug mixtures, Figures 1, 3, 5, 7, 9, 11, 13, 15, 17, 19 and 21 include plots of CI_{50} versus fraction of drug A, and Figures 2, 4, 6, 8, 10, 12, 14, 16, 18, 20 and 22 are corresponding plots, which are traditional isobolograms at the 50% effect level. Figures 1 to 8 show the effect of varying each of the polynomial coefficients, one at a time, with typical small to moderate effects on CI_{50} and isobols. Figures 9 to 12 represent more extreme patterns in CI_{50} and isobols caused by changes in only one polynomial coefficient. Figures 13 to 22 show complex profiles for CI_{50} and isobols, using sets of polynomial coefficients listed in Table 1.

Figures 23 and 24 show the effects of various values of β_{m12} and γ_{m12} on m. Figures 25 and 26 are examples of complex patterns for m, using sets of polynomial coefficients listed in Table 2.

Finally, we simulated examples for three-drug mixtures. Figure 27 includes several ternary plots for CI_{50} for various δ_{D123} values. Figure 28 has different examples of complex ternary plots for CI_{50}, for the corresponding sets of polynomial coefficients listed in Table 3. And, Figure 29 includes several ternary plots for m for various δ_{m123} values.

4.1. Two-drug mixtures

4.1.1. Characterization of CI_{50}

First we changed the values of α_{D1}, from -10 to 10 in increments of 1, with the other polynomial coefficients in Equation 5 fixed at zero. In Figure 1, one can see the resulting plot of CI_{50} (log scale) versus fraction of drug A, and in Figure 2, one can see the corresponding traditional isobol plot. The CI_{50} plots and isobols are purely synergistic for negative values of α_{D1} (below the CI_{50} = 1 additivity line) and purely antagonistic for positive values.

Table 3. Polynomial coefficients for complex CI50 patterns with three drugs

	Ternary Plot Label				
Parameter	Ex. A	Ex. B	Ex. C	Ex. D	Ex. E
α_{D1}	0	0	-2	-3	6
α_{D2}	0	0	-5	-1	3
α_{D3}	0	0	-4	-2	5
δ_{D123}	-130	130	230	-80	-270

The table lists the polynomial coefficients used for simulating the CI_{50}s in Figure 28 with equation 7. Labels ex. A to ex. E are for the different ternary plots in the figure.β and γ coefficients are always fixed at 0 for these examples

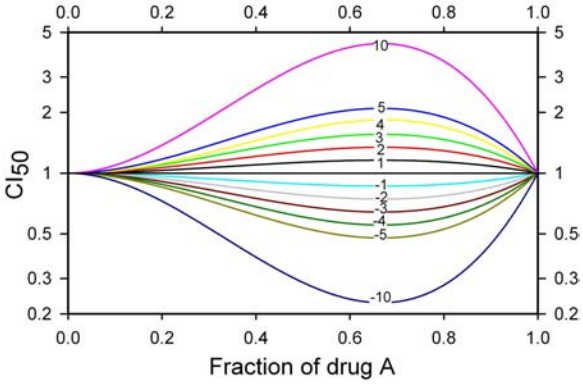

Figure 1. The effect of changing α_{D1} on CI_{50}. CI_{50} values (log scaled) versus normalized fraction of drug A. CI_{50} values are obtained by simulating CI_{50} with equation 5 for various values of α_{D1} (value indicated in the middle of the respective simulated curve). Other polynomial coefficients are fixed at zero. The uninterrupted horizontal black straight line is the additivity line (α_{D1} = 0; CI_{50} = 1).

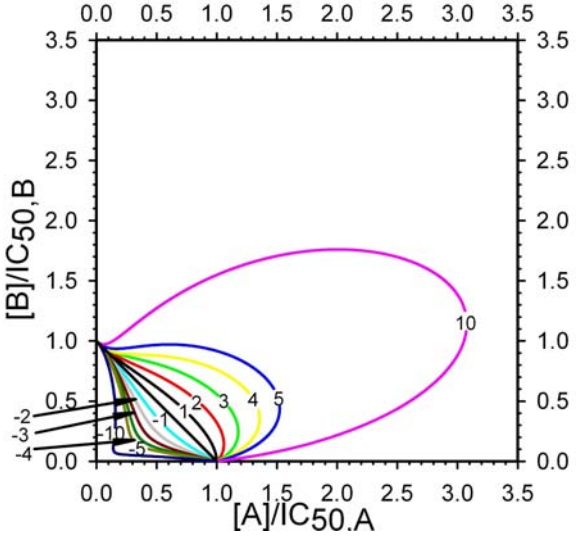

Figure 2. The effect of changing α_{D1} on CI_{50}. Isobologram at the 50% effect level corresponding to the CI_{50} plot in Figure 1. The diagonal black straight line from 1 to 1 is the additivity line (α_{D1} = 0).

When α_{D1} is at -10, -1, 1 and 10, the most extreme CI_{50} will be at 0.23, 0.86, 1.16 and 4.40, respectively. The most extreme CI_{50}s all occur at a fraction of drug A of 0.67. The plots are asymmetrical (skewed toward higher proportions of drug A) relative to a vertical axis at a fraction of drug A of 0.5 for the top panel, and relative to the NE to SW diagonal line for the isobol. Note that the isobol plots are not symmetrical, and that the shape of the synergistic isobols (below the NW to SE diagonal line from (0,1) to (1,0)) differs from that of the antagonistic isobols (above the line of additivity).

If we change α_{D2} (Figures 3-4), from -10 to 10 in increments of 1, with the other polynomial coefficients in Equation 5 fixed at zero, we get the mirror images of Figures 1-2.

When we change β_{D12} (Figures 5-6) from -10 to 10 in increments of 1, with the other polynomial coefficients in Equation 5 fixed at zero, we obtain a symmetric figure (relative to a vertical axis at a fraction of drug A of 0.5) or a symmetric isobol (relative to the NE to SW diagonal). As with the previous polynomial coefficients, the CI_{50} plots and isobols are purely synergistic for negative values of β_{D12} (below the CI_{50} = 1 additivity line) and purely antagonistic for positive values. When β_{D12} is at -10, -1, 1 and 10, the most extreme CI_{50} will be at 0.54, 0.94, 1.06 and 1.87, respectively. The most extreme CI_{50}s all occur at a fraction of drug A of 0.5. Note that the shape of the synergistic isobols (below the NW to SE diagonal line from (0,1) to (1,0)) is not the same as the antagonistic isobols (above the line of additivity).

Finally, we change γ_{D12} (Figures 7-8) from -10 to 10 in increments of 1, with the other polynomial coefficients in Equation 5 fixed at zero. The CI_{50} plots and isobols are first antagonistic (above the CI_{50} = 1 additivity line) then synergistic (below the CI_{50} = 1 additivity line) for negative values of γ_{D12}; and first synergistic then antagonistic for positive values. The switching point between antagonism and synergy is always for a fraction of drug A of 0.5. The absolute value of the vertical distance between the highest point of the curve (upper panel) and the horizontal additivity line (CI_{50} = 1) is always the same as the absolute vertical distance between the lowest point and the horizontal additivity line. When γ_{D12} is at -10/10, and -1/1, the most extreme CI_{50} will be at 0.98/1.02 and 0.84/1.20, respectively. The most extreme CI_{50}s all occur at fractions of drug A of 0.28 and 0.72. Note that the isobol plots are not symmetrical, and that the shape of the synergistic isobols (below the NW to SE diagonal line from (0,1) to (1,0)) differs from that of the antagonistic isobols (above the line of additivity).

Figures 9-10 and Figures 11-12 show patterns for extreme antagonism or extreme synergy respectively, using large values of each of the polynomial coefficients, one at a time, while the other polynomial coefficients are fixed at zero. We wanted to show CI_{50}s around 100 or 0.01as representative examples of extreme antagonism or synergy. For extreme antagonism, we had to raise α_{D1} to 31, or α_{D2}

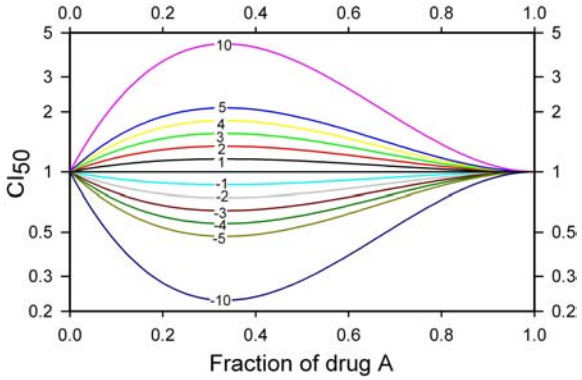

Figure 3. The effect of changing α_{D2} on CI_{50}. Details are the same as or analogous to those in Figure 1

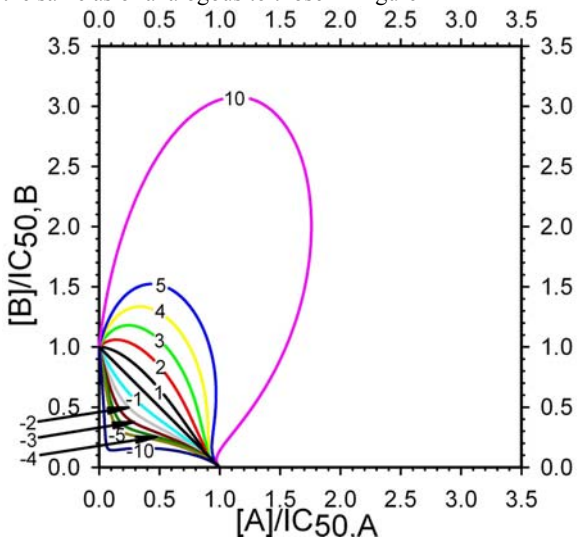

Figure 4. The effect of changing α_{D2} on CI_{50}. Isobologram at the 50% effect level corresponding to the CI_{50} plot in Figure 3

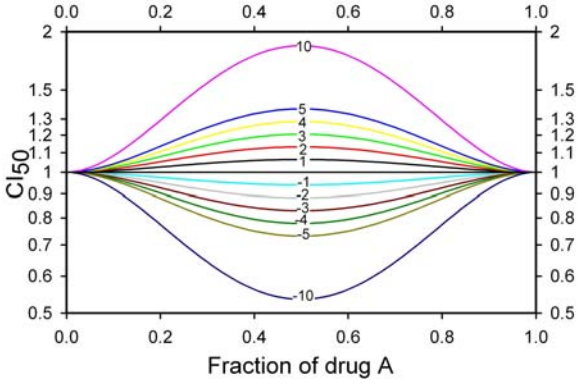

Figure 5. The effect of changing β_{D12} on CI_{50}. Details are the same as or analogous to those in Figure 1.

to 31, or β_{D12} to 73, or γ_{D12} to 255 (or lower to -255). For extreme synergy, we had to lower α_{D1} to -31, or α_{D2} to -31, or β_{D12} to -73, or γ_{D12} to -255 (or raise to 255).

Figure 13 to Figure 22 show examples of complex profiles, the lists for the sets of polynomial coefficients used are in Table 1. Figures 13-14 (curves A1 to A6) show examples of synergy with two local peaks of synergy. To obtain such profiles, we assigned negative values to α_{D1} and α_{D2}, and large values to γ_{D12} (the sign of γ_{D12} did not matter).

Figures 15-16 (curves B1 to B6) are the complements of Figures 14-15 for antagonism.

Figures 17-18 (curves C1 to C4) show composite profiles, with both asymmetrical local synergy and antagonism. The values of the parameters, α_{D1}, α_{D2}. β_{D12} and γ_{D12}, that generated curves C1 to C4 are listed in Table 1.

Figures 19-20 (curves D1 to D4) show seesaw patterns, with antagonism, then synergy, then antagonism (D1 and D4), or synergy, then antagonism, and then synergy (D2 and D3). The values of the parameters, α_{D1}, α_{D2}. β_{D12} and γ_{D12}, that generated curves D1 toD4 are listed in Table 1.

Figures 21-22 (curves E1 and E2) also show a seesaw pattern, but a symmetrical one (relative to a vertical axis at a fraction of drug A of 0.5 for the CI50 plot, and relative to the NE to SW diagonal line for the isobol), in contrast with Figures 19-20. α_{D1} and α_{D2} were always of the same sign, β_{D12} was of the opposite sign, and γ_{D12} was fixed at zero.

We could not obtain patterns that resulted in the CI_{50} line crossing the additivity line three times or more. If such a pattern would be needed to model real data, then it would be necessary to modify or augment the polynomials.

4.1.2. Characterization of m

α_{m1} and α_{m2} are simply the m's for drug A alone and drug B alone.

Figure 23 shows m versus the fraction of drug A for α_{m1} and α_{m2} fixed at -2, γ_{m12} fixed at 0, and β_{m12} ranging from -10 to 7 in increments of 1. Each resulting curve is symmetrical relative to a vertical line at a fraction of drug A of 0.5, and the curves with negative β_{m12} values are symmetrical to the curves with positive β_{m12} values, relative to a horizontal line at an m value of –2: curves with positive β_{m12} values are above the m = -2 line, curves with negative β_{m12} values are below the m=-2 line. If β_{m12} is equal to -10, the extreme value for m is -4.5; if β_{m12} is equal to 7, the extreme value for m is -0.25. The extreme values for m are observed at a fraction of drug A of 0.5. If β_{m12} is higher than 7, the highest value of m would be positive, which is incompatible with the kind of real data that we want to model.

Figure 24 represents m versus the fraction of drug A for α_{m1} and α_{m2} fixed at 2, β_{m12} fixed at 0, and γ_{m12} ranging from -10 to 10 in increments of 1. The plots are first below the m=-2 horizontal line, then above for

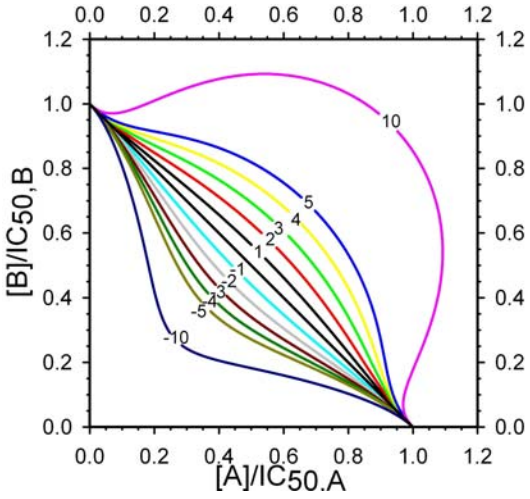

Figure 6. The effect of changing β_{D12} on CI_{50}. Isobologram at the 50% effect level corresponding to the CI_{50} plot in Figure 5

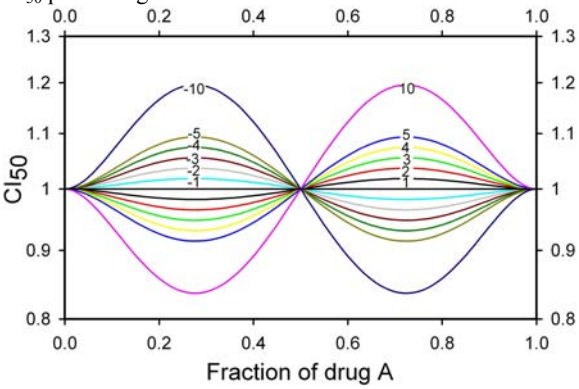

Figure 7. The effect of changing γ_{D12} on CI_{50}. Details are the same as or analogous to those in Figure 1

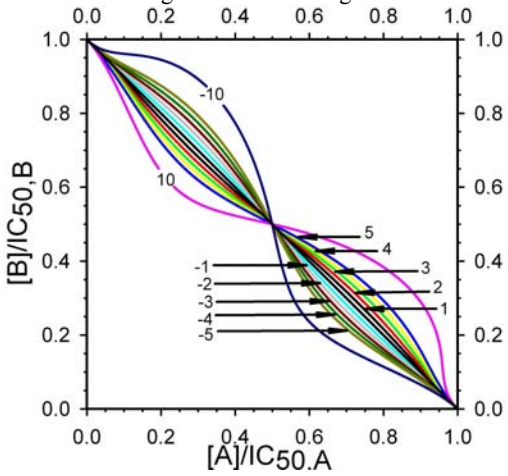

Figure 8. The effect of changing γ_{D12} on CI_{50}. Isobologram at the 50% effect level corresponding to the CI_{50} plot in Figure 7.

positive values of γ_{m12}; and first above then below for negative γ_{m12} values. The switching point between above and below the m=-2 line is always for a fraction of drug A of 0.5. The absolute vertical distance between the highest point and the horizontal m=-2 line is always the same as the absolute vertical distance between the lowest point and the horizontal m=-2 line. The extreme values of m are reached for fractions of drug A at 0.21 and 0.79. If γ_{m12} is equal to 10 or -10, the extreme values for m are -1.04 and -2.96.

Figure 25 and Figure 26 are examples of complex m profiles; the values of the polynomial coefficients used are listed in Table 2.

Figure 25 (curves A1 to A4) includes examples of profiles for m ranging to more extreme values than either m for the individual drugs alone. Drug A has a steepness parameter (m) of -0.5 and drug B has an m of -2 for profiles A1 and A2; A1 has as a minimum below -2 and A2 a maximum above -0.5. Drug A has a slope of -2 and drug B a slope of -0.5 for profiles A3 and A4; A3 has as a minimum below -2 and A4 a maximum above -0.5. β_{m12} and γ_{m12} are always of opposite signs, and β_{m12} is negative for the two curves with minimums below -2 (A1 and A3) but positive for the two curves with maximums above -0.5 (A2 and A4).

Figure 26 (curves B1 to B4) includes examples of curves where the m shifts rapidly from the slope of one drug alone to the slope of the other drug alone.

4.2. Three-drug mixtures

4.2.1. Characterization of CI_{50}

To represent the different values of CI_{50} for various values of polynomial coefficients for 3-drug mixtures, we used ternary plots. In these plots, each axis represents a normalized fraction of the drug in the mixture. The colors represent the simulated values for the CI_{50}s; the log-scaled color scheme is shown on the left side: red indicates synergy, yellow indicates additivity, and blue indicates antagonism.

Figure 27 shows an example of the effect of various δ_{D123} values on CI_{50}. The other polynomial coefficients are fixed at the following values: α_{D1} =-3, α_{D2} =12, α_{D3} =-8, β_{D12} =3, β_{D13} =2, β_{D23} =-15, γ_{D12} =20, γ_{D13} =-34, γ_{D23} =8. δ_{D123} was varied from -80 to 80 in increments of 40. The fixed polynomial coefficients have been chosen so that, on the "edges" of the ternary plots, we would have the following patterns:

- For the mixture of drug A and drug B, mostly antagonism, with small synergy for high fractions of drug A.
- For the mixture of drug A and drug C, pure synergy, but with an irregular isobol.
- For the mixture of drug B and drug C, first synergy (for low proportions of drug B) then antagonism (for high proportions of drug B), crossing the additivity line at the fraction of drug B of 0.5.

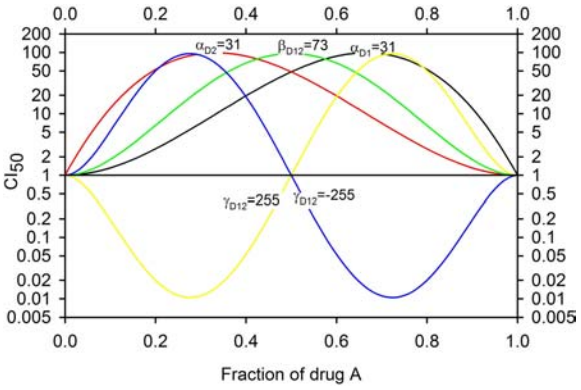

Figure 9. Extreme profiles of CI_{50} part A. CI_{50} values (log scaled) versus normalized fraction of drug A. The values of the polynomial coefficients are indicated on each single curve, unmentioned polynomial coefficients are by default fixed at zero. The uninterrupted horizontal black straight line is the additivity line (CI_{50} = 1).

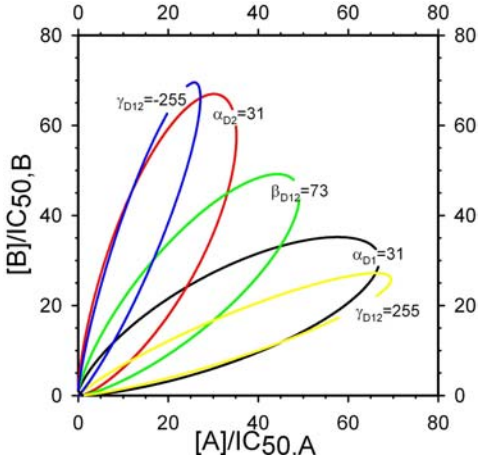

Figure 10. Extreme profiles of CI_{50} part A. Isobologram at the 50% effect level corresponding to the CI_{50} plot in Figure 9. The diagonal black straight line from 1 to 1 is the additivity line.

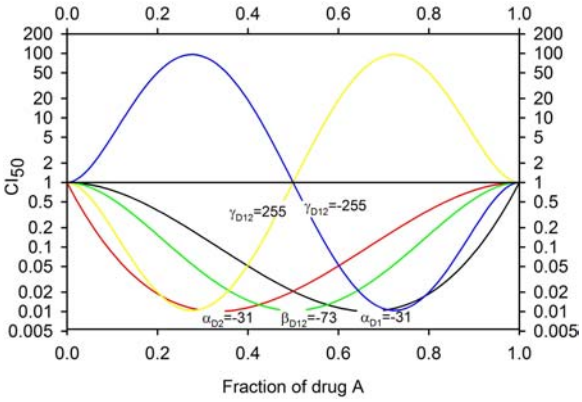

Figure 11. Extreme profiles of CI_{50} part B. Details are the same as or analogous to those in Figure 9.

When δ_{D123} is negative and decreases, the antagonistic area (blue region) increases while the synergistic area (red region) decreases; on the contrary, when δ_{D123} is positive and increases, the antagonistic area decreases while the synergistic area increases.

Figure 28 includes five examples of representative patterns for CI_{50}. The values of the sets of various polynomial coefficients are summarized in Table 3. β and γ coefficients were fixed at 0 for these examples.

Example A shows additivity for the three two-drug mixtures and synergy for the three-drug mixture. We can model this with α parameters fixed at zero, and a negative δ_{D123}.

Example B shows additivity for the three two-drug mixtures and antagonism for the three-drug mixture. We can model this with α parameters fixed at zero, and a positive δ_{D123}.

Example C shows synergy for the three two-drug mixtures and antagonism for the three-drug mixture. We can model this with negative α parameters, and a positive δ_{D123}, higher than in example B.

Example D shows synergy for the three two-drug mixtures and even more intense synergy for the three-drug mixture. We can model this with negative α parameters, and a negative δ_{D123}, lower than in example A.

Example E shows antagonism for the three two-drug mixtures and synergy for the three-drug mixture. We can model this with positive α parameters, and a negative δ_{D123}.

4.2.2. Characterization of m

Figure 29 shows examples of the effect of various δ_{m123} values on m. δ_{m123} was varied from -40 to 40 in increments of 20.The other polynomial coefficients were fixed at the following values: α_{m1}=-0.5, α_{m2}=-2, α_{m3}=-5, β_{m12}=-2.5, β_{m13}=2.5, β_{m23}=-10, γ_{m12}=-2, γ_{m13}=6, γ_{m23}=6. Yellow colors indicate slopes around -2; red colors are for slopes increasing toward -0.5, and blue colors indicate values of -5 and below -5.

The fixed polynomial coefficients have been chosen so that the m of drug A alone would be –0.5, m of drug B alone would be –2, m of drug C alone would be -5, and on the "edges" of the ternary plots, we would have the following patterns:

- For the mixture of drug A and drug B, m plateaus at –2 (m of drug B alone) for low and medium fractions of drug A, and changes to –0.5 (m of drug A alone) abruptly, only for high fractions of drug A.
- For the mixture of drug A and drug C, m changes progressively from –5 (m of drug C alone) to –0.5 (m of drug A alone) with increasing fraction of drug A, but also dips to around –0.3 before coming back to –0.5.

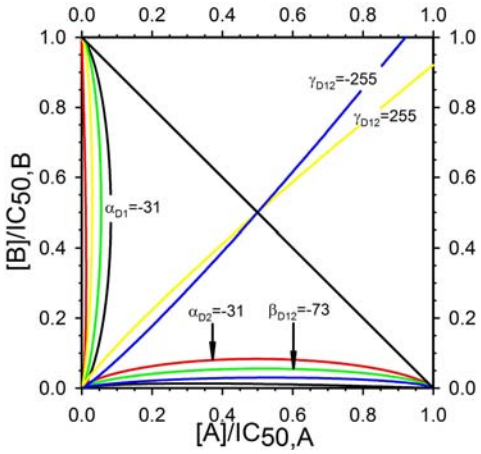

Figure 12. Extreme profiles of CI_{50} part B. Isobologram at the 50% effect level corresponding to the CI_{50} plot in Figure 11.

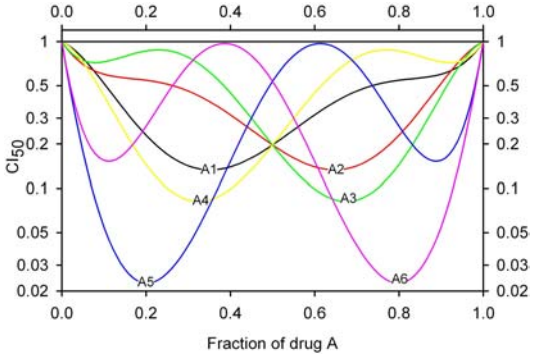

Figure 13. Complex profiles of CI_{50} part A. CI_{50} values (log scaled) versus normalized fraction of drug A. Each curve is named A1 through A6 in the figure. The polynomial coefficients are detailed in Table 1 for each curve. The uninterrupted horizontal black straight line is the additivity line (CI_{50} = 1).

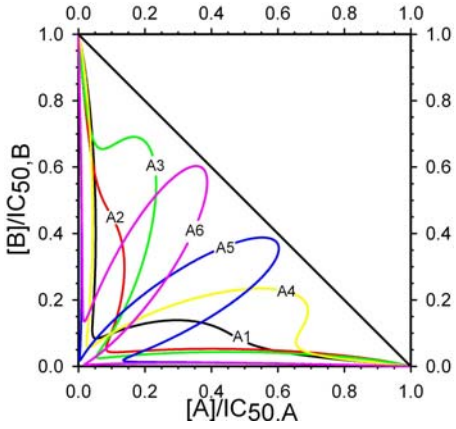

Figure 14. Complex profiles of CI_{50} part A. Isobologram at the 50% effect level corresponding to the CI_{50} plot in Figure 13. The diagonal black straight line from 1 to 1 is the additivity line..

- For the mixture of drug B and drug C, m changes rapidly from -5 (m of drug C alone) to –6.5, and then dips slowly to -2 (m of drug B alone).

When δ_{m123} is negative and decreases, the region with extreme ms (blue, ms below -5) increases, while when δ_{m123} is positive and increases, the region with ms closer to zero (red) increases.

4.3. Comparison with the Minto model

For our comparison, we considered the following polynomial equations from Minto *et al.* (8):

For m (Equation 8)

$$m(\mathbf{X},\boldsymbol{\theta}) = m_A + [(m_B - m_A - \beta_{2,m} - \beta_{3,m} - \beta_{4,m}) * X_B] + (\beta_{2,m} * X_B\text{^}2) + (\beta_{3,m} * X_B\text{^}3) + (\beta_{4,m} * X_B\text{^}4)$$

For CI_{50}: (Equation 9)

$$CI_{50}(\mathbf{X},\boldsymbol{\theta}) = 1 + [(-\beta_{2,D} - \beta_{3,D} - \beta_{4,D}) * X_B] + (\beta_{2,D} * X_B\text{^}2) + (\beta_{3,D} * X_B\text{^}3) + (\beta_{4,D} * X_B\text{^}4)$$

Here m_A and m_B are the slopes for drug A and drug B alone respectively, and $\beta_{2,m}$, $\beta_{3,m}$, $\beta_{4,m}$, $\beta_{2,D}$, $\beta_{3,D}$, and $\beta_{4,D}$ are the polynomial parameters.

For our simulations, we fixed m_A and m_B to -2, and we changed the six polynomial parameters mentioned above from -10 to 10 in increments of 1 when doable (we had to have negative values for m, and positive values for CI_{50}). The simulations are shown in Figure 30 (changing $\beta_{2,m}$), Figure 31 (changing $\beta_{3,m}$), Figure 32 (changing $\beta_{4,m}$), Figure 33 (changing $\beta_{2,D}$), Figure 34 (changing $\beta_{3,D}$), and Figure 35 (changing $\beta_{4,D}$) respectively.

First, it is to be noted that Minto *et al.* suggest using a polynomial function for the parameter characterizing the endpoint (effect) at infinite drug concentrations, that we called the background, B in this article. In our datasets, whether with antifungals (7) or anticancer drugs (6), we observed that a step function for B was more appropriate than a polynomial function.

For both the m and the CI_{50} simulations of the Minto model, we could observe that the curves were systematically biased toward the left (lower proportions of drug A). It is not a big problem for two-drug combinations as inverting A and B as needed could take care of this, but it will be more problematic for three-drug mixtures. We observe also that no single parameter allows immediately "seesaw" patterns, with curves going from one side of the additivity line or the m_A to m_B line to the other. In our model, this was made possible by the gamma parameters, γ_{D12} and.γ_{m12}. Finally, in the Minto *et al.* article (8), no specific parameter was mentioned for three-drug interactions, that could have been compared with our delta parameter.

For the polynomials for the slope m, the first parameter $\beta_{0,m}$ had to be constrained to be equal to m_A, like

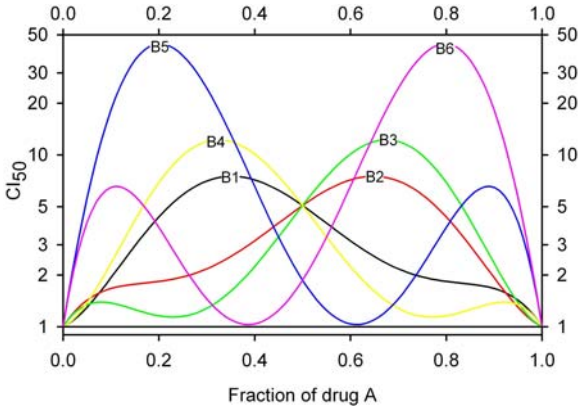

Figure 15. Complex profiles of CI_{50} part B. Details are the same as or analogous to those in Figure 13.

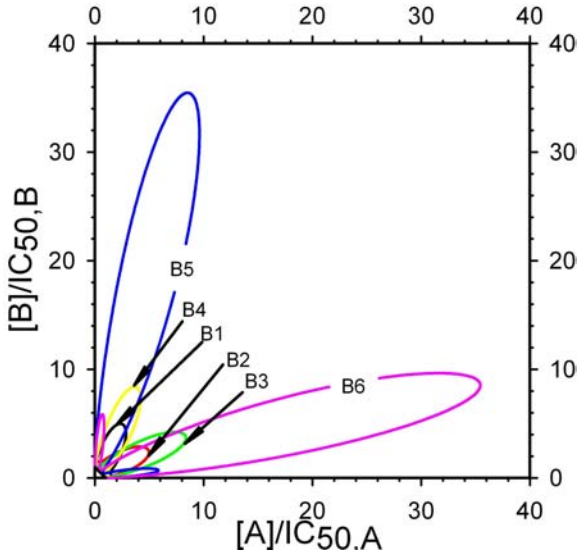

Figure 16. Complex profiles of CI_{50} part B. Isobologram at the 50% effect level corresponding to the CI_{50} plot in Figure 15.

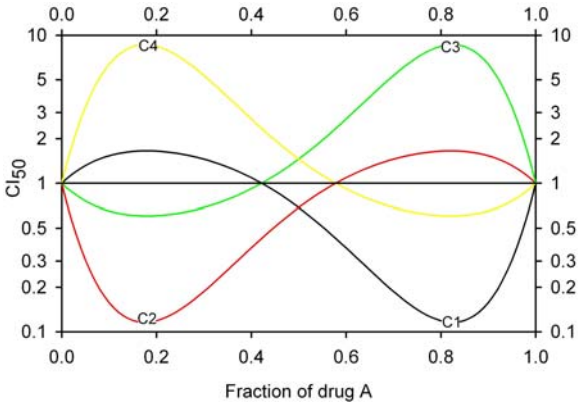

Figure 17. Complex profiles of CI_{50} part C. Details are the same as or analogous to those in Figure 13.

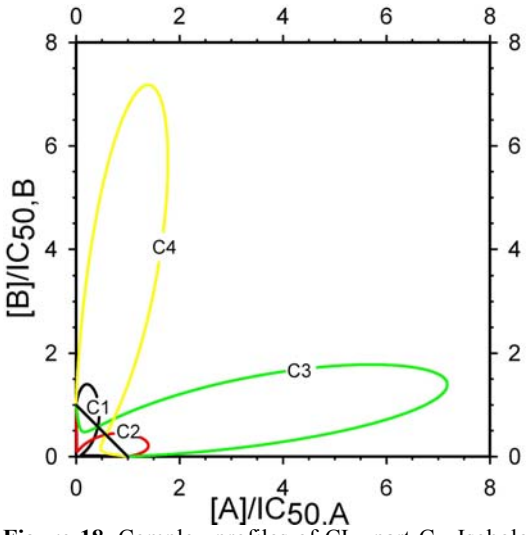

Figure 18. Complex profiles of CI_{50} part C. Isobologram at the 50% effect level corresponding to the CI_{50} plot in Figure 17.

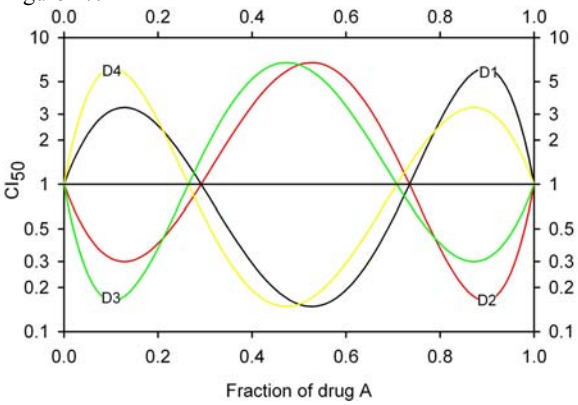

Figure 19. Complex profiles of CI_{50} part D. Details are the same as or analogous to those in Figure 13.

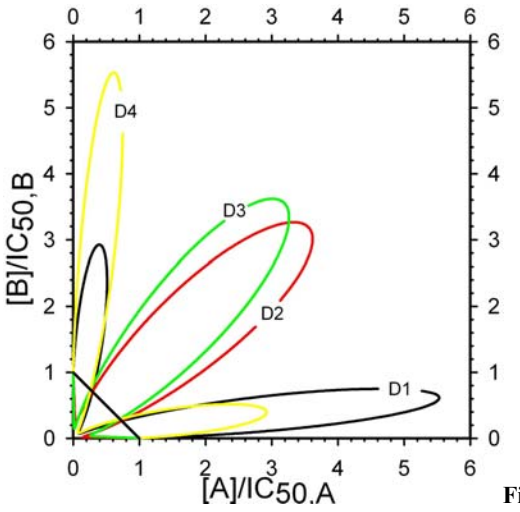

Figure 20. Complex profiles of CI_{50} part D. Isobologram at the 50% effect level corresponding to the CI_{50} plot in Figure 19.

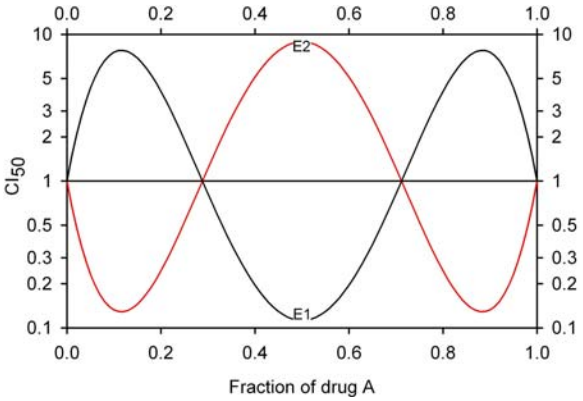

Figure 21. Complex profiles of CI_{50} part E. Details are the same as or analogous to those in Figure 13.

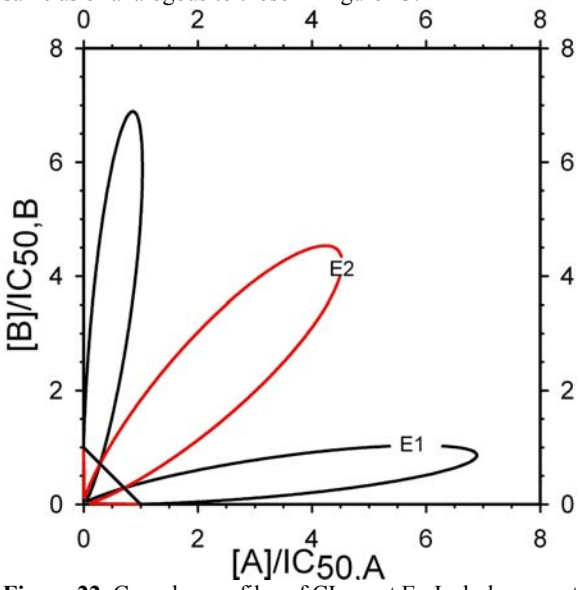

Figure 22. Complex profiles of CI_{50} part E. Isobologram at the 50% effect level corresponding to the CI_{50} plot in Figure 21.

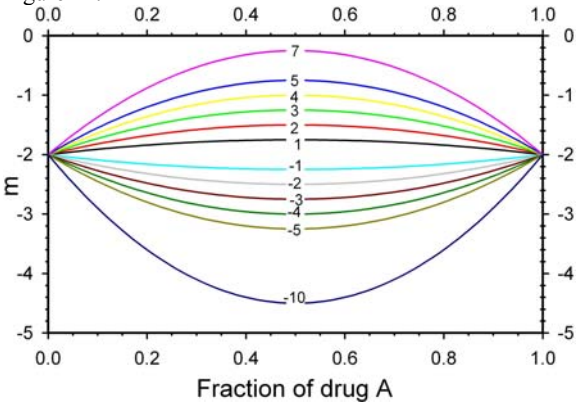

Figure 23. The effect of changing β_{m12} on m. m versus normalized fractions of drug A. m values are obtained by simulating m with equation 4 for various values of β_{m12}. α_{m1} = -2, α_{m2} = -2 and γ_{m12} = 0. The value of β_{m12} is indicated on the simulated curve.

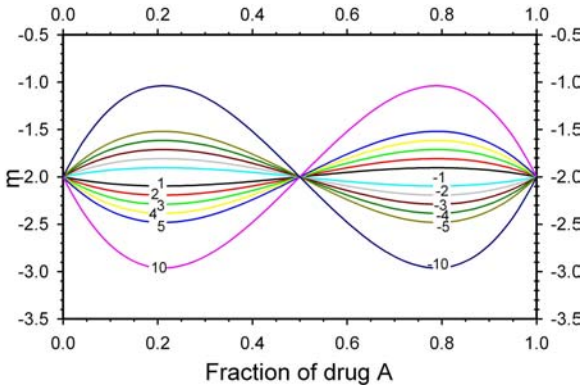

Figure 24. The effect of changing γ_{m12} on m. Details are the same as or analogous to those in Figure 23. α_{m1} = -2, α_{m2} = -2 and β_{m12} = 0.

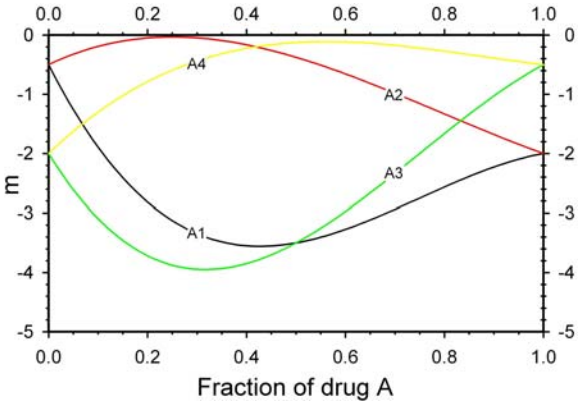

Figure 25. Complex profiles of m part A. m versus normalized fractions of drug A. Each curve is named A1 through A4 in the figure. The polynomial coefficients are detailed in Table 2 for each curve.

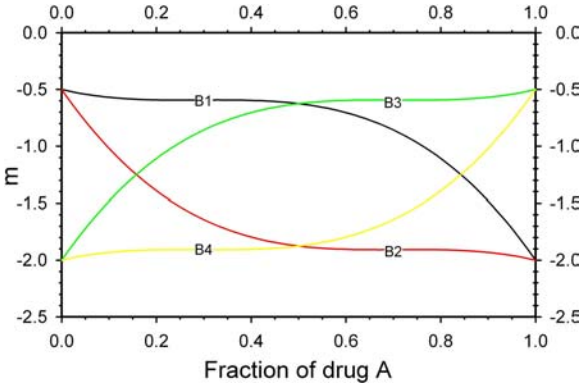

Figure 26. Complex profiles of m part B. Details are the same as or analogous to those in Figure 25.

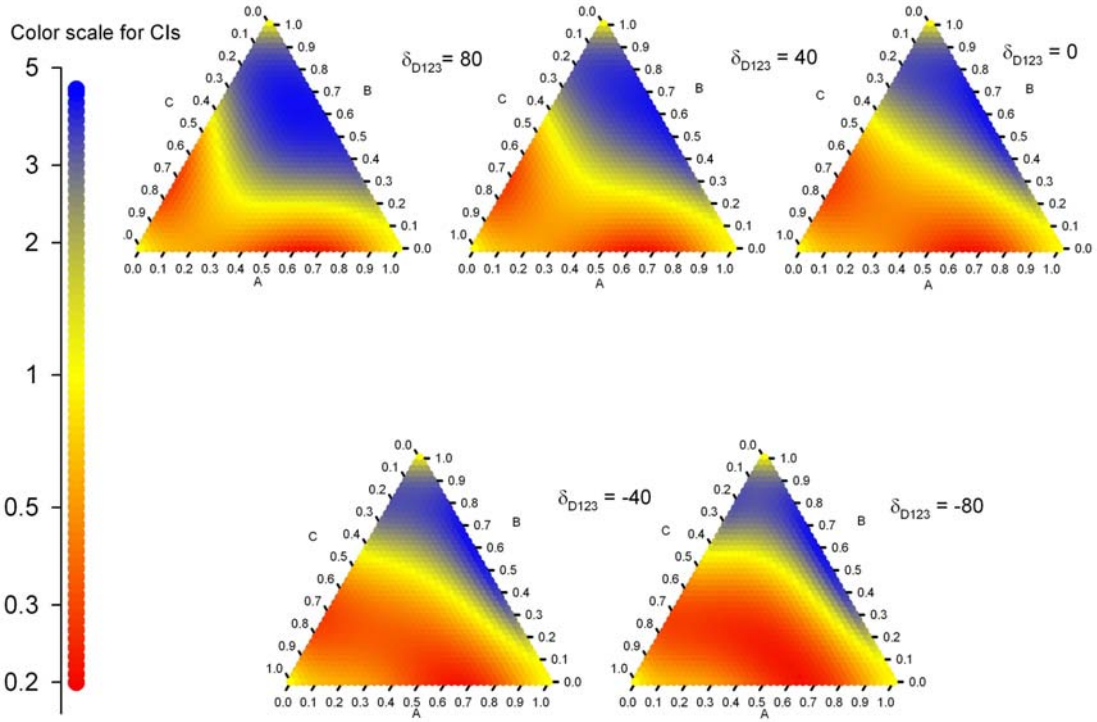

Figure 27. The effect of changing δ_{D123} on CI_{50}. Ternary plots represent the values of CI_{50} (according to the log-scaled color scale on the left side) versus normalized fractions of three drugs. CI_{50} values are obtained by simulating CI_{50} with equation 7, the various values of δ_{D123} are indicated on the side of the ternary plots. α_{D1} =-3, α_{D2} =12, α_{D3} =-8, β_{D12} =3, β_{D13} =2, β_{D23} =-15, γ_{D12} =20, γ_{D13} =-34, γ_{D23} =8.

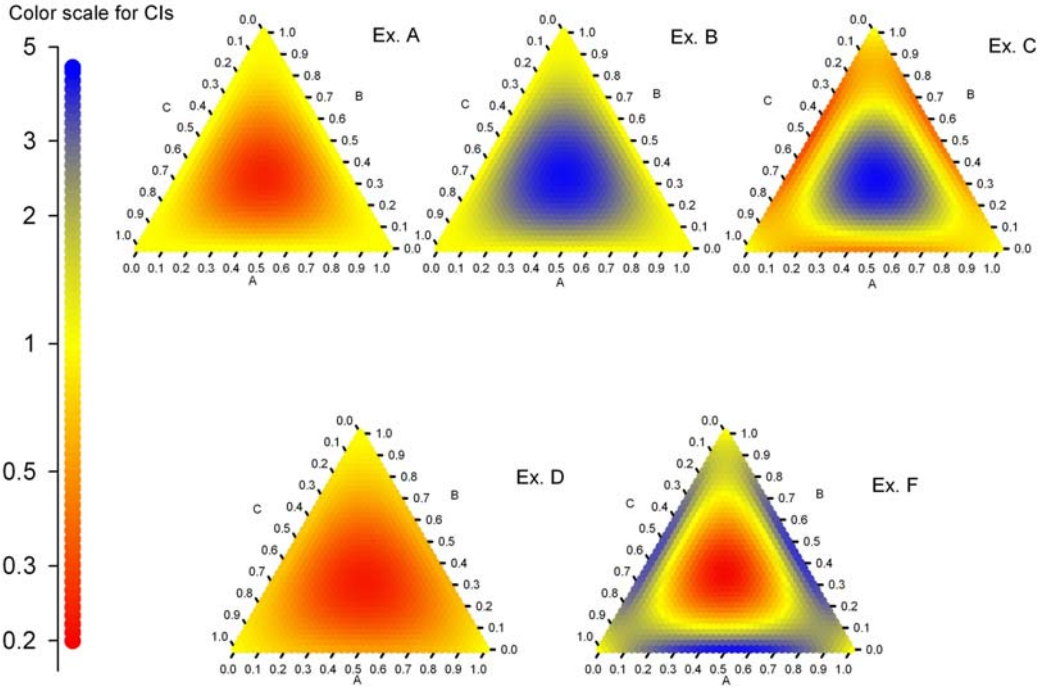

Figure 28. Various examples of ternary plots for CI_{50}. Ternary plots represent the values of CI50 (according to the log-scaled color scale on the left side) versus normalized fractions of three drugs. CI_{50} values are obtained by simulating CI_{50} with equation 7. The polynomial coefficients are described in Table 3, each ternary plot having its label on the side.

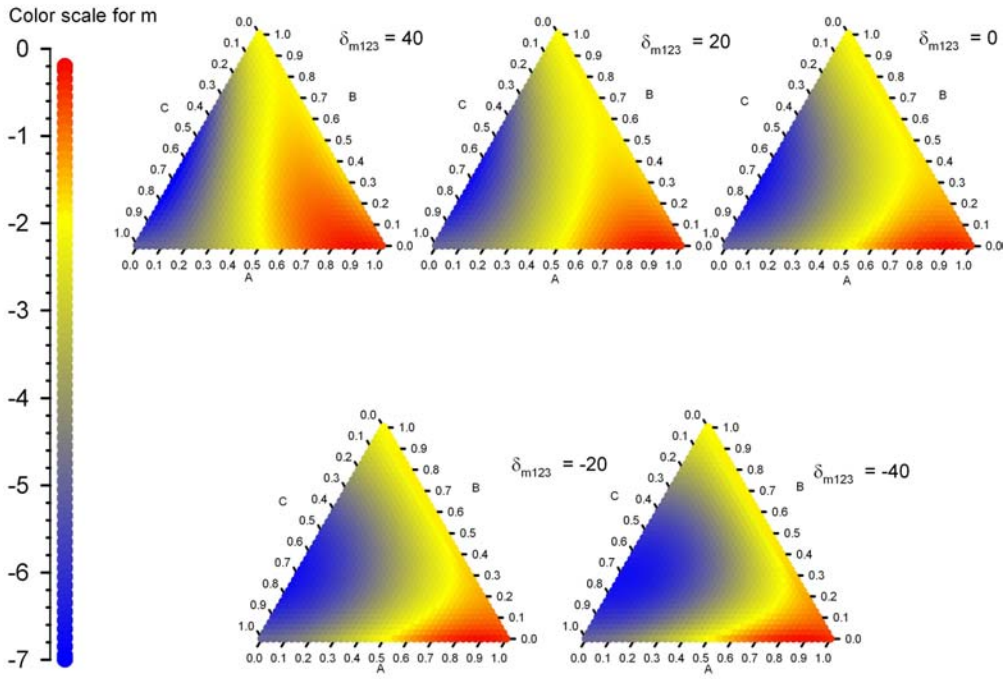

Figure 29. The effect of changing δ_{m123} on m. Ternary plots represent the values of m (according to the color scale on the left side) versus normalized fractions of three drugs. m values are obtained by simulating m with equation 6, the various values of δ_{m123} are indicated on the side of the ternary plots. α_{m1} =-0.5, α_{m2} =-2, α_{m3} =-5, β_{m12} =-2.5, β_{m13} =2.5, β_{m23} =-10, γ_{m12} =-2, γ_{m13} =6, γ_{m23} =6.

our parameter α_{m1}. The second parameter $\beta_{1,m}$, however, had to be constrained to be equal to m_B-m_A-$\beta_{2,m}$-$\beta_{3,m}$-$\beta_{4,m}$, and no parameter reflects directly m_B as our parameter β_{m1} does, making it less intuitive than our polynomial equation for steepness (sigmoidicity).

For the polynomials for CI_{50}, the first parameter $\beta_{0,D}$ had to be constrained to be equal to 1, and the second parameter $\beta_{1,D}$ had to be constrained to be equal to -$\beta_{2,D}$-$\beta_{3,D}$-$\beta_{4,D}$ so that the profiles would be anchored at 1 for the drugs alone. Our use of the leading factor $(1-X_A)*(1-X_B)$ and the power function provides this anchoring, without constraining any parameter. Also, it is to be noticed that Minto's polynomial for CI_{50} is not logarithmic, in contrast to ours. By its inherent mathematical and statistical nature, the CI_{50} parameter is most probably deserving of a logarithmic transformation, before expressing it as a polynomial function. Finally, since CI_{50} has to have only positive values, this limits the values that the different parameters may take in the Minto model; whereas, the polynomial coefficients (parameters) from the White model have no such constraints.

4.4. Conclusion

In conclusion, our model was reasonably flexible. Regarding the potency parameter CI_{50}, we could model simultaneous synergy and antagonism for the same two-drug mixtures, and even more so for the three-drug mixtures, with different kind of patterns, with many local pockets of synergy and antagonism. For m, we could model many different relevant geometrical shapes.

However, some limitations were found. In particular, for two agents, we could not obtain patterns that resulted in the CI_{50} curve crossing the additivity line three times or more. And for m, we could only barely approach a sharply changing profile.

On the other hand, our group made a decision, based upon practical experience working with several complex 3-agent datasets (5, 6), that the maximum practical complexity for the two critical polynomials should be equations 4,5 for two agents and equations 6,7 for three agents.

The decision was based on problems in interpreting the meaning of each individual coefficient in a very large set of polynomial coefficients, and the lack of practical interest by biologists in an extremely complex, but mostly empirical model. Our compromise approach is to limit the maximum complexity of the two critical polynomials. Note that also when fitting the White model to real data, polynomial coefficients with 95% confidence intervals that initially include zero will be likely removed from the model for subsequent curve fittings. Thus, for example, the final model for a three-drug mixture, may end up with less than the 10 total parameters illustrated in this article.

Overall, equations 1-3,6-7 comprise a response surface concentration-effect model that has been shown to be adequate and useful for fitting three different examples

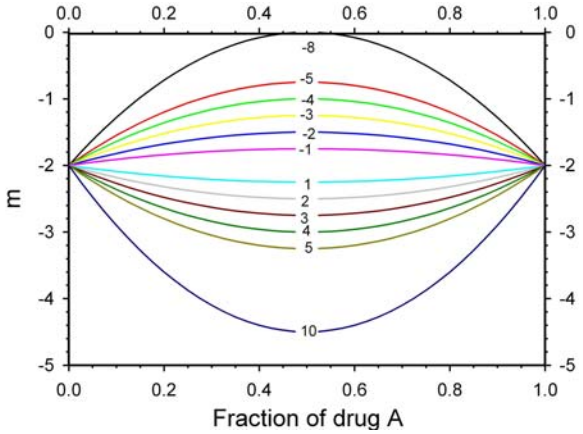

Figure 30. The effect of changing $\beta_{2,m}$ on m. m values versus normalized fraction of drug A. m values are obtained by simulating m with equation 8 for various values of $\beta_{2,m}$. Other polynomial coefficients are fixed at zero, m_A and m_B are fixed at -2. The value of $\beta_{2,m}$ is indicated on the simulated curve.

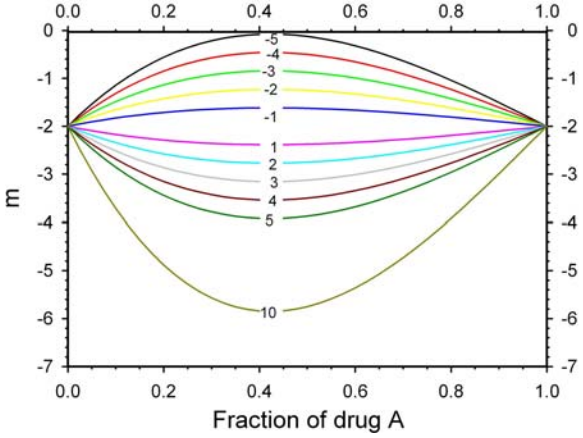

Figure 31. The effect of changing $\beta_{3,m}$ on m. Details are the same as or analogous to those in Figure 30.

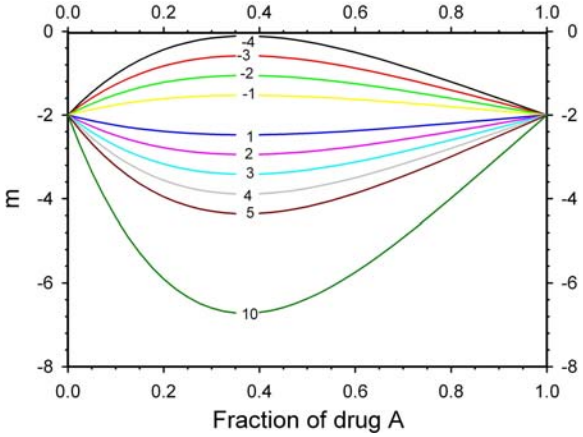

Figure 32. The effect of changing $\beta_{4,m}$ on m. Details are the same as or analogous to those in Figure 30.

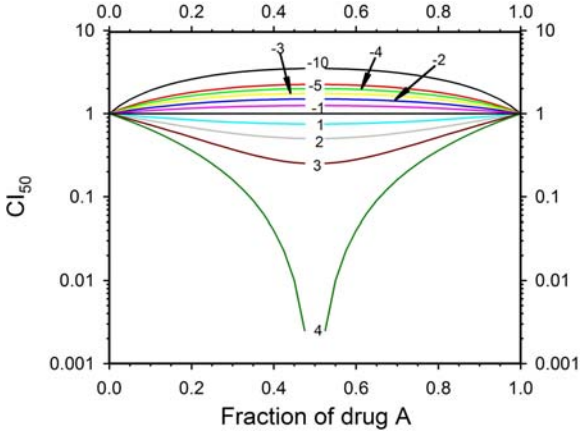

Figure 33. The effect of changing $\beta_{2,D}$ on CI_{50}. CI_{50} values versus normalized fraction of drug A. CI_{50} values are obtained by simulating CI_{50} with equation 9 for various values of $\beta_{2,D}$. Other polynomial coefficients are fixed at zero. The value of $\beta_{2,D}$ is indicated on the simulated curve. The uninterrupted black line is the additivity line (CI_{50} = 1).

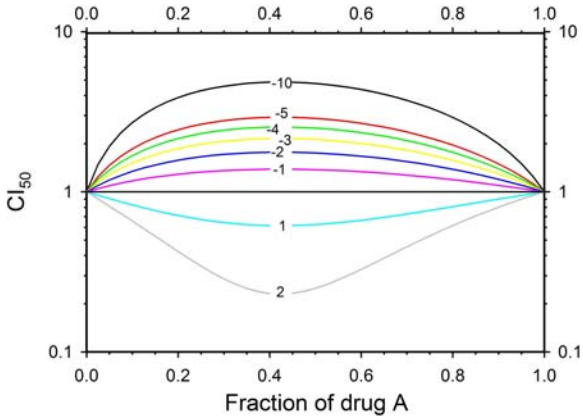

Figure 34. The effect of changing $\beta_{3,D}$ on CI_{50}. Details are the same as or analogous to those in Figure 33.

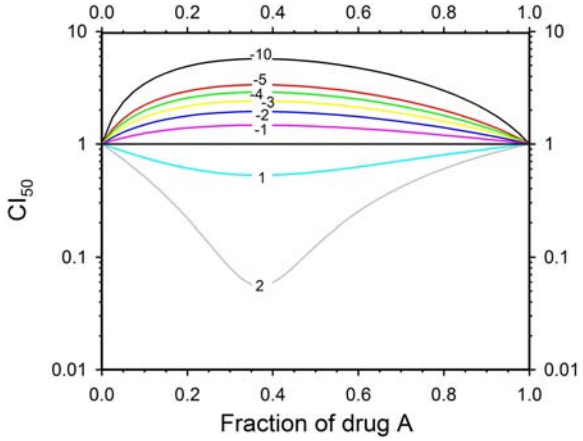

Figure 35. The effect of changing $\beta_{4,D}$ on CI_{50}. Details are the same as or analogous to those in Figure 33.

of very large, complex 3-agent data sets (5-7). The general modeling paradigm has enough flexibility to follow complex, observed patterns of sigmoidicity (m) and normalized potency (CI_{50}) versus drug fraction. Compared to the Minto model (8), the White model appears to include material improvements. The White model should be useful for a wide spectrum of future applications. Like all models, this response surface model has the potential to be improved.

5. ACKNOWLEDGMENTS

Supported in part by NIH RR10742 (WRG), and an educational grant from Novartis through the University at Buffalo, SUNY (YFB).

6. REFERENCES

1. Greco W.R., G. Bravo, J.C. Parsons: The search for synergy: a critical review from a response surface perspective. Pharm Rev 47, 221-285 (1995)

2. Berenbaum M.C.: What is Synergy? Pharm Rev 41, 93-141 (1989)

3. Loewe S. H. Muischnek: Effect of combinations: mathematical basis of problem. Arch Exp Pathol Pharmacol 11, 313-326 (1926)

4. Greco W.R., H.S. Park Y.M. Rustum: An application of a new approach for the quantitation of drug synergism to the combination of cis-diamminedichloroplatinum and 1-beta-D-arabinofuranosylcytosine. Cancer Res 50, 5318-5327 (1990)

5. White D.B., H.K. Slocum, Y.F. Brun, C. Wrzosek W.R. Greco: A new nonlinear mixture response surface paradigm for the study of synergism: a three drug example. Curr Drug Metab 2, 399-409 (2003)

6. White D.B., H.M. Faessel, H.K. Slocum, L. Khinkis W.R. Greco: Nonlinear response surfaces and mixture experiment methodologies applied to the study of synergism. Biometrical J 46, 56-71 (2004)

7: Brun Y.F., C.G. Dennis, W.R. Greco, R.J. Bernacki, P.J. Pera, J.J. Bushey, R.C. Youn, D.B. White B.H. Segal: Modeling the combination of Amphotericin B, Micafungin, and Nikkomycin Z against Aspergillus fumigatus *in vitro* using a novel response surface paradigm. Antimicrob Agents Chemother 51, 1804-1812 (2007)

8: Minto C.F., T.W. Schnider, T.G. Short, K.M. Gregg, A. Gentilini S.L. Shafer: Response surface model for anesthetic drug interactions. Anesthesiol 92, 1603-1616 (2000)

Key Words: Synergy Additivity Antagonism, Review

Send correspondence to: William Greco, 545 Hochstetter Hall, School of Pharmacy and Pharmaceutical Sciences, University at Buffalo, SUNY, Buffalo NY, 14260, Tel: 716-645-2842, ext 232, E-mail: rosgreco@hotmail.com

http://www.bioscience.org/current/vol2S.htm